MODELING OF TWO-PHASE FLOW IN A BWR FUEL ASSEMBLY WITH A HIGHLY-SCALABLE CFD CODE

Adrian Tentner, Prasad Vegendla, Aleks Obabko, Ananias Tomboulides, Paul Fischer, Oana Marin, Elia Merzari
Argonne National Laboratory
9700 S. Cass Avenue, Argonne, Illinois, USA 60439
tentner@anl.gov

ABSTRACT

A project is underway to develop an advanced two-phase flow modeling capability for the highly-scalable high-performance CFD code NEK5000 [1]. The goal of the project is to develop a new two-phase version of the NEK5000 code, named NEK-2P, to simulate the two-phase flow and heat transfer phenomena that occur in a Boiling Water Reactor (BWR) fuel bundle under various operating conditions. The NEK-2P two-phase flow models will follow the approach used for the Extended Boiling Framework [2, 3, 4] previously developed at Argonne, but will include more fundamental physical models of boiling phenomena and advanced numerical algorithms for improved computational accuracy, robustness, and computational speed.

The NEK-2P code is being developed on the foundation of the NEK5000 CFD Code developed at Argonne which provides general high-fidelity single-phase flow modeling capabilities. The paper describes the model development strategy which has been adopted by the development team for the simulation of two-phase boiling flow phenomena typical for a BWR fuel bundle. This strategy includes the extension of NEK5000 solver to allow modeling of two-phase boiling flows, and the implementation of an Advanced Boiling Framework (ABF) using local inter-phase surface topology maps and topology-specific phenomenological models. Results of initial analyses of selected experiments focused on boiling flow in a pipe with heated wall are presented.

KEYWORDS
Two-Phase Flow, Computational Fluid Dynamics, Boiling Flow Regimes, Boiling Water Reactor

1. INTRODUCTION

It is highly desirable to understand the detailed two-phase flow phenomena inside a BWR fuel bundle. These phenomena include coolant phase changes and multiple flow regimes which directly influence the coolant interaction with fuel assembly and, ultimately, the reactor performance. Traditionally, the best analysis tools for the simulation of two-phase flow phenomena inside the BWR fuel assembly have been the sub-channel codes. However, the resolution of these codes is too coarse for analyzing the detailed intra-assembly flow patterns, such as flow around a spacer element. Recent work in Computational Fluid Dynamics (CFD) including the initial implementation of the Extended Boiling Framework in the CFD code STAR-CD, showed promising potential for the fine-mesh, detailed simulation of fuel assembly two-phase flow phenomena.

The Extended Boiling Framework (EBF) [2, 3, 4] was developed for the fine-mesh, 3-dimensional simulation of the two-phase flow phenomena that occur in a Boiling Water Reactor (BWR) fuel assembly.

These phenomena include coolant phase changes and multiple flow topologies that directly influence the reactor performance. The EBF boiling models, which describe the inter-phase mass, momentum, and energy transfer phenomena specific for various local flow topologies, allow the simulation of a wide spectrum of flow regimes expected in a BWR fuel assembly. An overview of these models is included below in Section 3.The EBF was initially developed as a specialized module built on the foundation of the CFD code STAR-CD [5]. An effort is underway to port the EBF to the high-performance high-fidelity CFD code NEK5000 [1] which has initially been developed for the simulation of single-phase incompressible flow and is being extended to provide general two-phase boiling flow modelling capabilities.

This paper describes the approach adopted for the development of the NEK-2P code which extends the NEK5000 capabilities to allow the simulation of two-phase boiling flow phenomena. The paper also describes the initial implementation and extension of the EBF methodology in the NEK-2P code and key two-phase flow phenomenological models. The EBF uses a local inter-phase surface topology map in conjunction with models for the inter-phase mass, momentum, and energy exchanges for the bubbly, droplet, and transition flow topologies. It also calculates the conjugate heat transfer using a wall heat transfer model that describes the heat exchange between the heated wall and the two-phase or single-phase coolant. Initial results of selected two-phase boiling flow experiment simulations are presented and compared with measured data.

2. THE TWO-PHASE CFD CODE NEK-2P

Nek5000 is a highly-scalable open-source transient CFD code developed at Argonne National Laboratory which has been recognized with the Gordon Bell prize in high-performance computing and has run on over one million processes on Argonne's massively parallel Blue Gene/Q computer Mira. The code is based on the spectral element method and it is written in basic FORTRAN and C languages. The original Nek5000 was built for the simulation of single phase constant-density flows. A later version of the code, referred to as the Low-Mach version, was modified to allow the simulation of single-phase variable-density perfect-gas flows. The project team decided to use the Low-Mach version of NEK5000 as the platform for the implementation of two-phase boiling modeling capabilities in Nek-2P. While a finite volume formulation is still being evaluated, the initial two-phase modeling capability is being implemented using the existing spectral method formulation. The development of the NEK-2P has followed a staged approach, beginning with the development of a homogeneous two-phase model and continuing with a more complex two-phase drift-flux model. The initial implementation of these two-phase models has been completed and their formulation and assumptions are described below. A parallel effort to develop a two-phase two-velocity model for NEK-2P is also underway which will be described in a future paper.

2.1. The Homogeneous Two-Phase Model of the NEK-2P code

Because only one velocity field is available in the Low-Mach version of NEK5000, we decided to begin with the implementation of a homogeneous two-phase model. The main assumptions of the homogeneous model are: a) the local velocities of the water and vapor phases are assumed to be the same for each computational element, and b) the local temperatures of the water and vapor phases are assumed to be the same for each computational node. The phase transition from water to vapor is due to local enthalpy changes which in a reactor fuel assembly or in a heated pipe experiment are driven by the wall heat flux. The mass, momentum, and energy conservation equations are shown below:

Continuity:

$$\frac{\partial \rho_m}{\partial t} + \nabla.(\rho_m \boldsymbol{u}_m) = 0 \tag{1}$$

Momentum:

$$\frac{\partial (\rho_m \boldsymbol{u}_m)}{\partial t} + \nabla.(\rho_m \boldsymbol{u}_m \boldsymbol{u}_m) = -\nabla p + \nabla.\boldsymbol{\tau} + \rho_m \boldsymbol{g} + \boldsymbol{F}_e \tag{2}$$

Enthalpy:

$$\frac{\partial (\rho_m h_m)}{\partial t} + \nabla.(\rho_m \boldsymbol{u}_m h_m) = \nabla.(k \nabla T_m) + Q \tag{3}$$

The above conservation equations are reformulated similar to the Low-Mach number equations of Nek5000 as described in [6].

Continuity:

$$\nabla.\boldsymbol{u}_m = -\frac{1}{\rho_m}\frac{\partial \rho_m}{\partial h_m}\frac{dh_m}{dt} \tag{4}$$

Momentum:

$$\rho_m \frac{\partial \boldsymbol{u}_m}{\partial t} + \rho_m \boldsymbol{u}_m.\nabla \boldsymbol{u}_m = -\nabla p + \nabla.\boldsymbol{\tau} + \rho_m \boldsymbol{g} + \boldsymbol{F}_e \tag{5}$$

Enthalpy:

$$\rho_m \frac{\partial h_m}{\partial t} + \rho_m \boldsymbol{u}_m.\nabla h_m = \nabla.(k \nabla T_m) + Q \tag{6}$$

The closure equations for the homogeneous two-phase model are given below:

Density [kg.m^{-3}]:

$$\rho_m = \rho_L(1-\alpha) + \rho_G \alpha \tag{7}$$

Thermal conductivity [W.m^{-1}.K^{-1}]:

$$k_m = k_L(1-\alpha) + k_G \alpha \tag{8}$$

Temperature [K]:

$$T_m = Tsat + \frac{(h_m - h_L)}{Cp_L}, \qquad [h_m < h_L] \tag{9}$$

$$T_m = Tsat, \qquad [h_L \leq h_m \leq h_G] \tag{10}$$

$$T_m = Tsat + \frac{(h_m - h_G)}{Cp_G}, \qquad [h_m > h_G] \tag{11}$$

The continuity, momentum, and enthalpy equations 4-6 are solved each time step based on the current two-phase mixture conditions. Subsequently, the phase volume fractions are updated based on the calculated enthalpy field at each location. In next iteration, the updated mixture properties (Equations 7-11), i.e., density, thermal conductivity, and temperature are used to solve continuity, momentum, and enthalpy equations. This iterative procedure is performed until the specified flow convergence criteria are met.

2.2. The Drift-Flux Two-Phase Model of the NEK-2P code

The development of the drift-flux model is an intermediate step in the development of the two-phase NEK-2P code. The approach selected by the development team is intended to extend the capabilities of the homogeneous two-phase model described above in a manner that minimizes the changes to the one-velocity two-phase solver and to provide a test-bed for the implementation of the Extended Boiling Framework while the two-velocity two-phase solver of the NEK-2P code is being developed.

The drift-flux model accounts for the effect of different vapor and liquid velocities within the framework of the one-velocity solver. The current model allows different phase velocities, but assumes that the liquid and vapor have the same temperature in each computational cell. The calculation of the local liquid and vapor velocities requires the use of the Extended Boiling Framework as described below. The NEK-2P solves for the two-phase mixture velocity, defined as:

$$\boldsymbol{u}_m = \frac{\boldsymbol{u}_L \times \rho_L \times (1-\propto) + \boldsymbol{u}_G \times \rho_G \times \propto}{\rho_m} \tag{12}$$

The vapor velocity $\mathbf{u}_G$ and liquid velocity $\mathbf{u}_L$ are related at each location by the local slip ratio $S_j = u_{j,G}/u_{j,L}$. To avoid potential numerical problems when a component of the liquid velocity becomes small, each slip ratio component is limited to a maximum value $S_j < S_{j,max}$. The conservation equations 4-6 are then re-formulated to reflect the effect of the different phase velocities:

Continuity:

$$\nabla . \boldsymbol{u_m} = -\frac{1}{\rho_m}\frac{\partial \rho_m}{\partial h_m}\frac{dh_m}{dt} \tag{13}$$

Momentum:

$$\rho_m \frac{\partial \boldsymbol{u}_m}{\partial t} + \boldsymbol{C}_{mom}\,\rho_m\,\boldsymbol{u}_m . \nabla \boldsymbol{u}_m + \boldsymbol{u}_m[-\nabla . (\rho_m \boldsymbol{u}_m) + \nabla . (\boldsymbol{C}_{mom}\,\rho_m \boldsymbol{u}_m)] = -\nabla p + \nabla . \mu \nabla \boldsymbol{u}_m + \rho_m\,\boldsymbol{g} + \boldsymbol{F}_e \tag{14}$$

Enthalpy:

$$\rho_m \frac{\partial h_m}{\partial t} + \mathbf{C}_{\text{enth}}\rho_m \boldsymbol{u}_m . \nabla h_m + h_m[-\nabla . (\rho_m \boldsymbol{u}_m) + \nabla . (\mathbf{C}_{\text{enth}}\rho_m \boldsymbol{u}_m)] = \nabla . (k \nabla T_m) + Q \tag{15}$$

The field constants $\boldsymbol{C}_{mom}$ and $\boldsymbol{C}_{enth}$ are obtained from the derivation of the new transport equations 13-15 and are based on the gas-to-liquid velocity ratio S defined above:

$$C_{\text{j},mom} = \rho_m \frac{\alpha_G \rho_G S_j^2 + \alpha_L \rho_L}{\left(\alpha_G \rho_G\, S_j + \alpha_L \rho_L\right)^2} \tag{16}$$

$$C_{\text{j},enth} = \frac{\alpha_G \rho_G h_G S_j + \alpha_L \rho_L h_L}{h_m\,(\alpha_G \rho_G S_j + \alpha_L \rho_L)} \tag{17}$$

The NEK-2P solver updates the mixture velocity defined in Equation 14 every time step, without accounting for the effect of the interphase forces. The vapor and liquid velocities ($\boldsymbol{u}_G^*$ *and* $\boldsymbol{u}_L^*$) based on the updated mixture velocity are then updated accounting for the effect of the inter-phase forces during the time step (equations 18-21). The local inter-phase forces $\mathbf{F}_\text{i}$ are calculated using the local inter-phase surface topology defined by the Extended Boiling Framework described in Section 3 below. The updated vapor and liquid velocities ($\boldsymbol{u}_G^{new}$ *and* $\boldsymbol{u}_L^{new}$) are used to update the local slip ratio S used to calculate the coefficients C_{mom} and C_{enth} in equations 16 and 17 above.

$$\Delta \boldsymbol{u}_G = \frac{\sum \boldsymbol{F}_i}{\alpha_G \rho_G}\,dt \tag{18}$$

$$\boldsymbol{u}_G^{new} = \boldsymbol{u}_G^* + \Delta \boldsymbol{u}_G \tag{19}$$

$$\Delta \boldsymbol{u}_L = -\frac{\sum \boldsymbol{F}_i}{\alpha_L \rho_L}\,dt \tag{20}$$

$$\boldsymbol{u}_L^{new} = \boldsymbol{u}_L^* + \Delta \boldsymbol{u}_L \tag{21}$$

3. THE ADVANCED BOILING FRAMEWORK

The calculation of the mass, momentum, and energy inter-phase interactions is based on the use of the Extended Boiling Framework [2, 3, 4] which has been implemented in NEK-2P and is reviewed in this section. The NEK-2P implementation of the EBF introduces new features that allow a more rigorous treatment of the inter-phase interaction terms in the transition region described in Section 3.1 below and is referred to as the Advanced Boiling Framework (ABF). A brief discussion of the new ABF features is included in Section 3.2 below. The EBF is used in the implementation of the drift-flux model described above and for the analysis of the subcooled boiling experiments described in Section 4. The transition from the EBF to ABF is underway and it is planed that the two-velocity two-phase NEK-2P solver currently under development will use the ABF.

3.1 Inter-phase Surface Topology Map and Local Flow Configuration

Inter-phase interactions in multiphase fluids depend on both the area and the topology of the phase interface. Sub-channel thermal-hydraulic codes rely on flow regime maps to evaluate the interface topology using cross-section-averaged flow parameters. CFD codes, which divide the flow space into much finer computational cells cannot rely on the traditional sub-channel flow regimes, but must evaluate instead the local inter-phase surface topology. The ensemble of many computational cells with relatively simple inter-phase surface topologies can provide complex global topologies that include all the traditional sub-channel flow regimes.

Most of the advanced CFD codes currently allow the simulation of dispersed flows only (bubbly or mist flows) where the flow topology is originally defined and remains the same in both space and time. This approach is applicable only to flows without topology changes and without sharp interfaces. Flow topology changes are typical for boiling flows in BWR fuel assemblies as illustrated schematically in Figure 1. Moreover, local sharp interfaces often exist in boiling flows, e.g., between Taylor bubbles and the near-wall film in slug flow, or between the gas core and the liquid film in annular-mist flow in heated pipes or rod bundles. The changing topology conditions typical for boiling flows in BWR fuel assemblies, including sharp-interface topologies such as the annular-mist flow regime, cannot be modeled accurately with topology-independent correlations used for inter-phase interactions in such flows. Meanwhile, it is essential to adequately describe these regimes in BWR channel simulations, since they govern near-wall film formation and evolution, which, in turn, determines important fuel assembly characteristics such as Critical Heat Flux (CHF) and wall dryout.

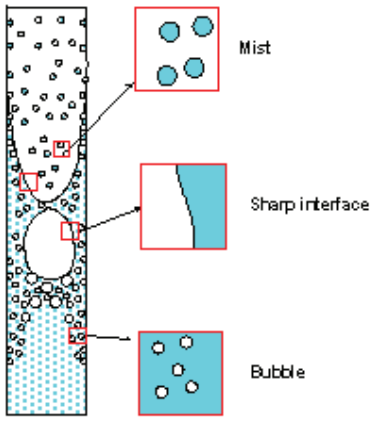

Figure 1 Schematic view of upward flow in vertical channel with heated walls

The EBF boiling model uses a locally calculated topology variable to allow the following topologies: a) a bubbly flow topology with spherical vapor bubbles in a continuous liquid, b) a droplet or mist topology with spherical liquid droplets flowing in a continuous vapor field, and c) a transition topology which combines the features of the two previous topologies in various proportions. The local topology is determined in this model using a local topology map based on the local void fraction. This 1-dimensional topology map is illustrated in Fig. 2 together with the associated flow topologies.

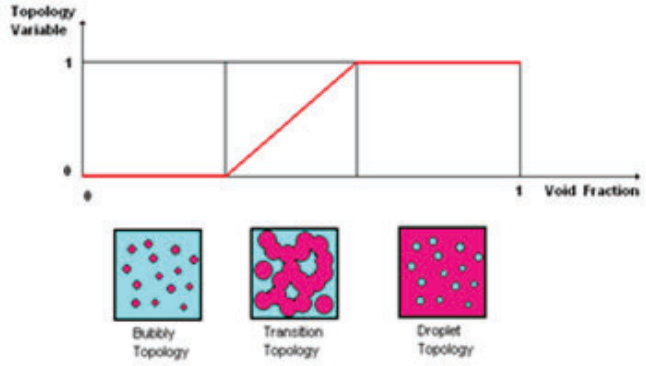

Figure 2 Inter-phase Surface Topology Map used for the Extended Boiling Framework

3.2 The wall-cell sharp-interface topology

The topology map discussed above does not address directly the presence of cells that contain a sharp single-connected interface, such as wall cells that contain a thin liquid film. Wall cells that satisfy specific conditions imposed on both the local void fraction and void fraction gradient are treated in the EBF boiling model as a special liquid film topology illustrated in Figures 3a and 3b. Because the EBF allows only one liquid and one vapor field in each cell, the wall cells can contain only a liquid film and vapor. As the liquid volume fraction decreases the liquid film, which initially covers the entire wall surface (Figure 3a) is assumed to become unstable and to cover the wall surface only partially (Figure 3b).

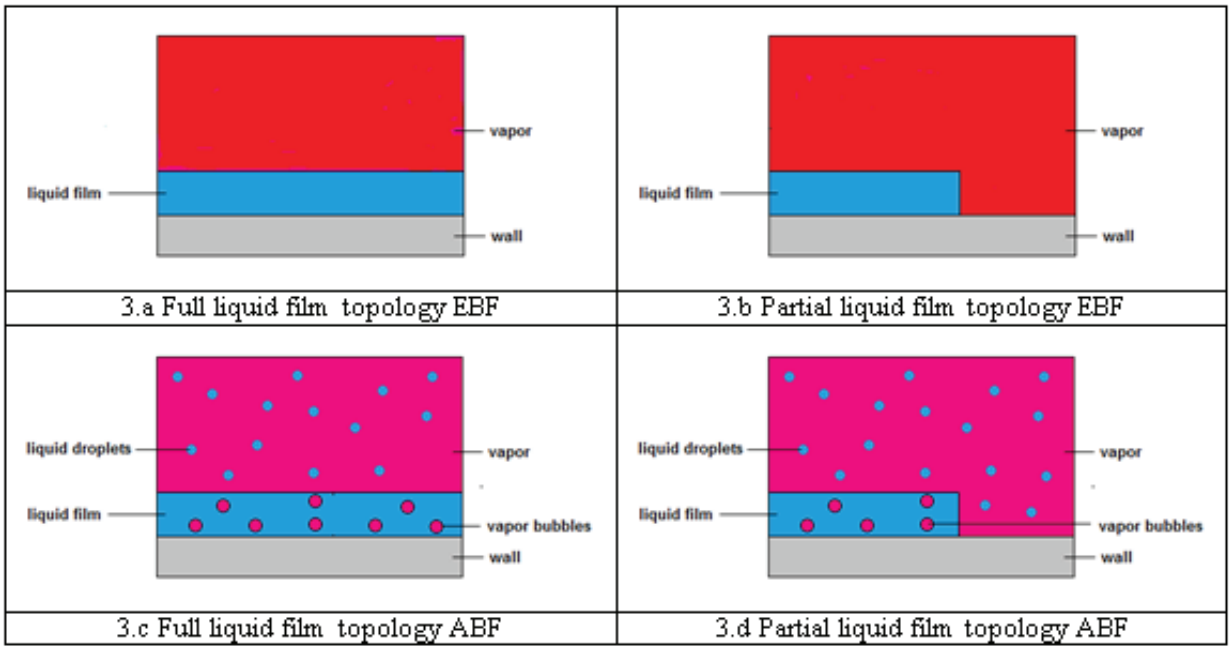

Figure 3: Wall cell topology in EBF and ABF

The ABF extends the EBF capabilities by allowing two liquid fields (continuous and dispersed) and two vapor fields (continuous and dispersed) in each computational cell. The ABF wall cell topologies corresponding to the EBF topologies discussed above are illustrated in Figures 3.c and 3.d. The liquid in the wall cell is now divided between the liquid film and the liquid droplets field. Because only one liquid velocity and one liquid temperature are defined for each cell, the droplet and film velocities and temperatures are the same. However, the partition of the liquid between the liquid film and droplets has important implications for the heat transfer between the heated wall and the two-phase coolant. The EBF wall-cell sharp-interface topology model has been shown to provide good predictions of wall temperature changes in STAR-CD EBF analyses of three CHF experiments [7] but later analyses of other CHF experiments with significantly different flow rates and/or wall heat flux have shown less satisfactory results. The ABF wall-cell sharp-interface topology model including the explicit modelling of the film entrainment and the partition of liquid between the film and droplets in the wall cells have been shown in STAR-CD ABF analyses of multiple CHF experiments to provide good predictions of wall temperature changes in CHF experiment analyses over a wide range of coolant flow rates and wall heat fluxes [8].

3.3 Inter-phase mass, momentum, and energy transfer models

The inter-phase surface topology map is used to evaluate the interfacial area and inter-phase interactions. Three basic local flow configurations with specific interface topology are identified (bubbly flow, mist flow and sharp interface) and the interfacial area and inter-phase mass, momentum, and energy transfer models are defined for these configurations. In the domain identified in Fig. 2 as transitional topology it is assumed that a combination of basic flow configurations is present, and the quantities required for closure are found by determining the appropriate combination of mass, momentum, and energy exchange terms for the local flow topology. The most general transitional topology is illustrated in Fig. 4, and various other transitional topologies are obtained by retaining only a sub-set of the master-cell features.

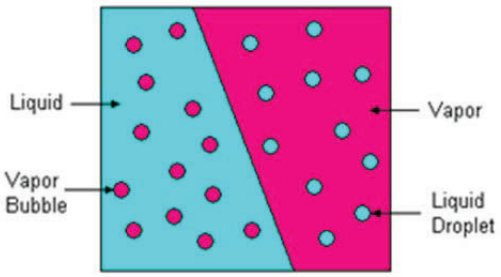

Figure 4: General transitional cell topology

As demonstrated in [9], the use of the local inter-phase surface topology map allows the modeling of complex sub-channel-scale topologies that emerge from combinations of many computational cells with one of the local topologies shown in Figures 2 and 3. E.g., the typical sub-channel annular flow regime could be resolved into a distinct core flow region in which the gas phase is continuous and the local mist topology is used, separated by transition topology cells from a liquid film on the wall where the local bubbly topology and the wall-cell topology are used.

4. RESULTS OF SELECTED BOILING FLOW EXPERIMENTS

An effort to validate the two-phase models that are being implemented in NEK-2P, the two-phase version of the NEK5000 code, has been initiated. The validation effort will rely on analyses of previous two-phase experiments available in the open literature or from collaborations with various experimental teams. The validation effort will also identify the need for additional CFD-quality two-phase boiling data that may require new two-phase flow experiments. The planned validation effort will include the analysis of multiple boiling flow experiments addressing a wide spectrum of two-phase flow phenomena relevant for reactor fuel bundles, following the approach used previously for the validation of the EBF models implemented in the STAR-CD code [11]. The experiment analyses presented in this section are only a first step in the NEK-2P validation effort and address a limited set of the two-phase flow phenomena of interest. It is noted, however, that they represent the first demonstration of the two-phase modeling capabilities implemented in the NEK-2P code.

4.1. Subcooled Boiling Flow Experiment Simulations

In this section, the homogeneous and drift-flux two-phase versions of NEK-2P are used to analyze a series of three subcooled boiling experiments performed by Bartolomei et al. [10]. These analyses are used to evaluate the performance of the bubbly-flow subcooled boiling models in the context of the NEK-2P homogeneous and drift-flux formulations. The Bartolomei experiments are subcooled boiling experiments performed in a vertical heated tube as shown in Figure 5. The diameter and length of the vertical pipe are 12.03 mm and 1.4m, respectively.

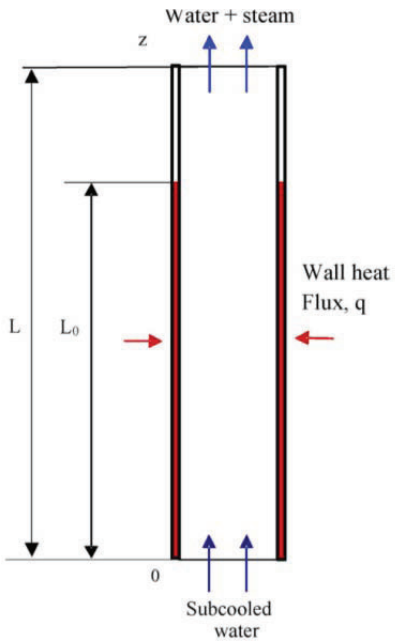

Figure 5: Schematic diagram of the Bartolomei experiment [9]

The experiments covered a wide range of wall heat fluxes and mass flow rates. In these experiments wall heating is applied only up to 1m of the pipe height, where water boiling occurs near the heated wall and consequently steam is generated. Some vapor condensation also occurs as the bulk of the flow remains

subcooled, but the total cross-section vapor volume fraction increases gradually. The rest of the tube wall, with a length of 0.4 m is in adiabatic condition. Only vapor condensation occurs in this section of the pipe due to the mixing of the vapor generated upstream near the heated wall with the sub-cooled liquid core. The operating conditions of the three experiments analyzed are shown in Table 1.

Table 1. Operating Conditions for the experiments analyzed

Experiments	Mass Flux [G: $kg/m^2.s$]	Wall Heat Flux [q_{wall}: W/m^2]	dT [K] (T_{in}-T_{sat})	q_{wall} /G
Exp#A	1000	80E4	55	800
Exp#B	1500	80E4	39	533
Exp#C	1500	120E4	63	800

The cross-section average void fraction calculated for these three experiments with the homogeneous and drift-flux two-phase models in NEK-2P are compared with the corresponding measured data in Figure 6. The results obtained in a previous analysis [11] of the Bartolomei experiments with the STAR-CD two-velocity model using the EBF model are also included for comparison. The void fraction distribution calculated with the NEK-2P drift-flux model for experiments A-C is shown in Figure 7.

The results shown in Figure 6 indicate that both the Homogeneous and Drift-Flux models implemented in NEK-2P describe reasonably well the vapor fraction evolution both in the heated section and in the adiabatic section of the pipe. A comparison of the results obtained with the homogeneous model as shown in Figure 6 indicates that the drift flux model results are generally closer to the measured data than those of the homogeneous model. This applies to the heated length of the pipe including the peak void fraction and to the adiabatic region of the pipe as well. The results of the NEK-2P drift flux model also generally closer to the experimental data than those obtained with the STAR-CD EBF models for all three experiments, with the exception of the heated section of the experiment C, where the void fraction calculated with STAR-CD follows closer the experimental results. It is also observed in Figure 6 that the NEK-2P boiling models predict a somewhat higher location for the onset of wall boiling than that observed in the experiments. This could be due to the assumption of liquid and vapor temperature equilibrium in each computational cell which is built into both the homogeneous and the drift flux models. The STAR-CD EBF results, which were obtained with a two-fluid model that allows intra-cell vapor-liquid temperature non-equilibrium, provide a more accurate prediction of the initial vapor formation location. We plan to explore the effect of vapor-liquid temperature non-equilibrium when the NEK-2P two-fluid model becomes available. It is noted that the inclusion of turbulence models in the NEK-2P homogeneous and drift-flux formulations is still underway. In this work the turbulence effects are included by increasing the liquid viscosity and thermal conductivity by a multiplying factor which is dependent on the radially averaged void fraction at each axial location, as shown in Table 2.

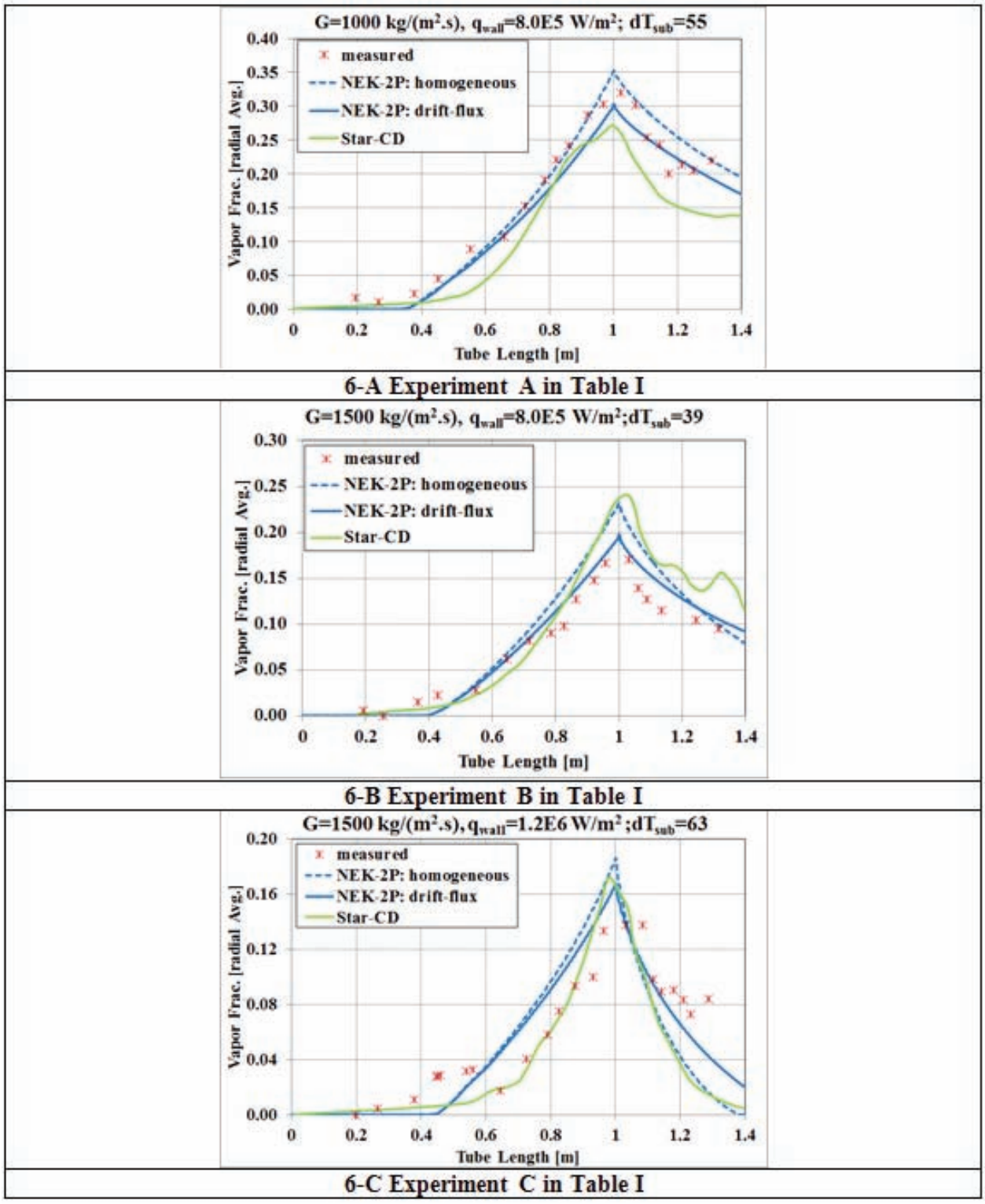

Figure 6 Radially-averaged vapor fraction profiles along the length of the pipe for the three experiments analyzed

Table 2 Multiplying factors for thermal conductivity and viscosity

Heated Section	Adiabatic Section
$0.08\ G_{in}\ .\ exp^{[5.0E^{-6}.q_{wall}.\propto.(1-\propto)]}$	$0.013\ G_{in}\ .\ exp^{[5.0E^{-6}.q_{wall}.\propto.(1-\propto)]}$

Where G_{in} is the inlet mass flux in Kg/(m^2-s), q_{wall} is the wall heat flux in W/m^2, and α is the radially averaged void fraction at a given axial location.

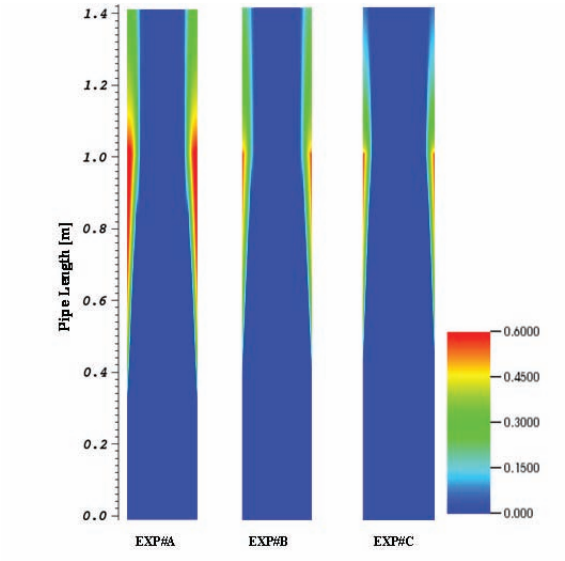

Figure 7 Vapor fraction distribution calculated with the NEK-2P two-phase drift-flux model in an axial cross-section of the three experiments analyzed

5. CONCLUSIONS

A project to develop an advanced two-phase flow modeling capability for the highly-scalable CFD code NEK5000 was described. The goal of the project is to develop a new two-phase version of the NEK5000 code, named NEK-2P, which will simulate a wide spectrum of two-phase flow and heat transfer phenomena that occur in a Boiling Water Reactor (BWR) fuel bundle under various operating conditions.

The paper described the status of the NEK-2P model development effort and the strategy adopted by the development team for the CFD simulation of two-phase boiling flow phenomena typical for a BWR fuel bundle. The NEK5000 solver has been extended to allow modeling of two-phase boiling flows. Both a homogeneous two-phase solver and a drift-flux two-phase solver have been implemented in NEK-2P. The drift-flux two-phase solver relies on the use of an Advanced Boiling Framework (ABF) which describes the inter-phase interactions using local inter-phase surface topology maps and topology-specific phenomenological models.

Results of initial NEK-2P analyses of several experiments focused on subcooled boiling flow in a pipe with heated wall are presented. The new NEK-2P drift-flux two-phase model provides a reasonably good description of the vapor void fraction evolution observed in the experiments, both in the heated region and the adiabatic region of the pipe. Some differences between the calculated and measured void fraction are observed in the low void region of the heated section of the pipe which are attributed to the assumption of intra-cell vapor and liquid temperature equilibrium used in the current two-phase models. This assumption will be removed in future work when the NEK-2P two-fluid model, which includes a two-temperature formulation, is completed. Future work is planned which will use the NEK-2P code to analyze multiple boiling flow experiments focused on a wide spectrum of two-phase flow phenomena relevant for LWRs.

NOMENCLATURE

C_p	Specific heat [J/kg.K]
d	diameter [m]
g	gravity [m/s^2]
G	mass flux [$kg/m^2.s$]
h	enthalpy [J/kg]
k	thermal conductivity [J/m.s.K]
F	force vector [N/m^3]
p	pressure [N/m^2]
q	heat flux [W/m^2]
Q	heat source [W/m^3]
S	velocity ratio [u_G/u_L]
t	time [sec]
T	temperature [K]
u	velocity vector [m/s]
α	vapor volume fraction
ρ	density [kg/m^3]
τ	shear stress [$kg/m.s^2$]

Subscripts:

G	vapor
in	inlet
L	liquid
m	mixture
sat	saturation
e	external
i	inter-phase
j	spatial coordinate index [x, y, z]

ACKNOWLEDGMENTS

Support for the development of the NEK-2P is provided by the U.S. DOE Office of Science.
Support for the initial development of the EBF was provided by the U.S. DOE GIPP Program.

REFERENCES

1. P. F. Fischer, J. Lottes, W.D. Pointer, A. Siegel. “Petascale algorithms for reactor hydrodynamics”, J. Phys. Conf. Series (2008)
2. A.Tentner, S.Lo, A.Ioilev, M.Samigulin, V.Ustinenko, Computational Fluid Dynamics Modeling of Two-phase Flow in a Boiling Water Reactor Fuel Assembly, Proc. Int. Conf. Mathematics and Computations, American Nuclear Society, Avignon, France, Sept. 2005.
3. A.Tentner, S.Lo, A.Ioilev, M.Samigulin, V.Ustinenko, V.Melnikov, V.Kozlov, Advances in computational fluid dynamics modeling of two phase flow in a boiling water reactor fuel assembly. Proc. Int. Conf. Nuclear Engineering ICONE-14, Miami, Florida, USA, July 17-20, 2006.
4. A.Tentner, W.D.Pointer, T.Sofu, D.Weber, Development and Validation of an Extended Two-Phase CFD Model for the analysis of Boiling Flow in Reactor Fuel Assemblies, Proc. Int. Conf. Advances in Nuclear Power Plants, Nice, France, May 13-18, 2007.
5. STAR-CD Version 3.20 Methodology Manual, Chapter 13, CD-adapco, UK. 2004.
6. A. G. Tomboulides, J. C. Y. Lee and S. A. Orszag. Numerical Simulation of Low Mach Number Reactive Flows**.** Journal of Scientific Computing. Vol. 12. No. 2. 1997
7. A. Ioilev, M. Samigulin, V. Ustinenko, P. Kucherova, A. Tentner, S. Lo, A. Splawski “Advances in the modeling of cladding heat transfer and critical heat flux in boiling water reactor fuel assemblies”, Proc. 12th International Topical Meeting on Nuclear Reactor Thermal Hydraulics (NURETH-12), Pittsburgh, Pennsylvania, USA, September 30-October 4, 2007
8. A.Tentner, E. Merzari, P. Vegendla, “Computational Fluid Dynamics Modeling of Two-Phase Boiling Flow and Critical Heat Flux”, Proceedings of ICONE22, the 22nd International Conference on Nuclear Engineering, Prague, Czech Republic, July 7-11, 2014.
9. A. Tentner, S. Lo, A. Splawski, A. Ioilev, V. Melnikov, M. Samigulin, V. Ustinenko,. "Computational Fluid Dynamics Modeling of Two-Phase Flow and Inter-Phase Surface Topologies in a BWR Fuel Assembly," Proceedings of ICONE16, the 16th International Conference on Nuclear Engineering, Orlando, FL, USA, May 11-15, 2008.
10. G.G. Bartolomei, G.N. Batashov, V.G. Brantov, V.G., et al. Teplomassoobmen-IV, vol. 5. Minsk. ITMO AN BSSR Press, Vol. 5, pp. 38 (1980).
11. V. Ustinenko, M. Samigulin, A. Ioilev, S. Lo, A. Tentner, A. Lychagin, A. Razin, V. Girin, Ye. Vanyukov. Validation of CFD-BWR, a new two-phase computational fluid dynamics model for boiling water reactor analysis. Nuclear Engineering and Design 238 (2008) 660–670